PREPARATION AND PROPERTIES OF Co-Fe MIXED OXIDES OBTAINED BY CALCINATION OF LAYERED DOUBLE HYDROXIDES

MARÍA E. PÉREZ BERNAL, RICARDO J. RUANO CASERO, VICENTE RIVES

Departamento de Química Inorgánica. Universidad de Salamanca, 37008-Salamanca, Spain

E-mail: vrives@usal.es

Solids containing Co(II) and Fe(III) with molar ratios of 2/1, 3/2, 1/1, 2/3 and 1/2 have been synthetised by coprecipitation at constant pH. All they displayed a hydrotalcite-like structure with interlayer carbonate, which crystallinity decreases as the iron content was increased. No other crystalline phase was identified, even in the Fe-rich samples. They have been characterised by powder X-ray diffraction, FT-IR spectroscopy, thermal analysis (differential thermal analysis, thermogravimetric analysis and temperature-programmed reduction), in addition to specific surface area assessment by nitrogen adsorption at -196°C. A minor oxidation of Co(II) to Co(III) is observed in the Co-rich samples, although it reverses again to Co(II) upon calcination in oxygen at ca. 850°C. Thermal decomposition takes place in a single step up to ca. 350°C, and the specific surface area increases with the iron content, probably because of the presence of hydrated amorphous iron oxides. The solids calcined at 1200°C in air contain crystalline CoO, Co_3O_4 and $CoFe_2O_4$ (spinel), this one being the dominant phase, and only phase detected for large Fe contents. Metallic species are more easily reduced in the original solids than in the calcined ones, and in all cases iron seems to be reduced at a higher temperature than cobalt.

INTRODUCTION

Layered double hydroxides (LDHs) with the hydrotalcite-like structure are deserving the interest of many research groups because of their use in many different fields, such as anions scavengers, catalysts, catalyst precursors, hosts for drugs controlled delivery, etc. [1]. Their structure consists of brucite-like layers, where a partial Mg^{2+}/Al^{3+} substitution has taken place, so anions are located in the interlayers (where water molecules also exist) to balance the positive charge of the layers. Their formula can be written as $[M^{II}_{1-x}M^{III}_x(OH)_2]A^{n-}_{x/n} \cdot mH_2O$, where A stands for the interlayer anion, which is carbonate in natural hydrotalcite and many other minerals and synthetic compounds with this structure, but many different anions have been intercalated following different routes [2,3]. On the other hand, the precise nature of the layer cations can be changed in a wide range, the limits being their molar ratio, and their ionic radii [4-6].

Although for applications in Medicine and environmental protection, LDHs containing Mg^{2+} and Al^{3+} are usually preferred because of their lack of toxicity, those with transition metal cations are generally used as catalysts or catalyst precursors [7-10] for mild and total oxidation, alcohol synthesis, hydroxylation, etc.

Among many other LDHs, we have previously reported on the synthesis and characterisation of LDHs containing Co and Fe in the layers and carbonate as the interlayer anion; the properties of the original and of the products calcined at different temperatures were reported [11], but such a study was restricted to solids with Co/Fe ratios ranging from 2.4 to 2.7 which corresponded to a crystallographic pure hydrotalcite. In the present work, we have dealt with solids with this same qualitative composition, but where the molar Co/Fe ratio ranged from 2 to 0.5, in order to analyse the formation of different mixed oxides upon calcination at high temperatures. It is foreseen that these solids may be used as catalysts for total oxidation of carbon monoxide and hydrocarbons.

EXPERIMENTAL

All reagents were from Panreac (Spain), PRS quality, and were used without any further purification. Gases were from L'Air Liquide (Spain). Solution A was prepared by dissolving Co(II) and Fe(III) chlorides (in preselected molar ratios) in water at room temperature at a total metal cation concentration of 2 M. Solution A was filtered to remove any trace of insoluble material

before addition to solution B. This one, containing sodium hydrogencarbonate (the stoichiometric amount corresponding to a Fe(III)/HCO$_3^-$ molar ratio of 1/1) and hydroxide (its amount that necessary to neutralize HCO$_3^-$ and that required to form the LDH), was cooled to room temperature for ca. 45 min after preparation before addition of solution A, and the ratio between the volumes of solutions B and A was 2/1. This solution was slowly added dropwise to solution B, which was being mechanically stirred at ca. 400 rpm with a model RZR-Z051 Heidolph stirrer; from the very first moment, formation of a brown precipitate was observed. Addition was completed after 3-4 h and then the suspension was stirred mechanically between 14-20 h at room temperature. The precipitate was filtered in a Büchner funnel (20 cm diameter) with a water pump. The cake was washed three times with portions of 150 ml and a fourth one with 500 ml of bidistilled water. The water pump was connected in all cases after 20 min standing the cake with the bidistilled water; the washing liquids were apparently colourless in all cases, with *pH* ranging from 9.4 to 9.9. After completing washing, air was passed through the cake for two hours and the powder then extended on glass sheets to dry them at room temperature and open air. After 4-5 days the samples were hand ground in an agate mortar. The samples are named as CoFe0x, where x = 1,2,3,4,5 correspond to molar Co/Fe ratios of 2/1, 3/2, 1/1, 2/3, and 1/2, respectively. The samples were brown, becoming slightly reddish as the iron content was increased.

A portion of each solid was calcined in a close furnace in air at 5°C/min up 1200°C, this temperature being maintained for 1 h (samples CoFe0x/1200).

Elemental chemical analysis for Co and Fe were carried out at Servicio General de Análisis Químico Aplicado (Universidad de Salamanca, Spain) in a Mark-II ELL-240 instrument by atomic absorption after proper dissolution of the samples in nitric acid.

Powder X-ray diffraction (PXRD) diagrams were recorded in a Siemens D-500 instrument, using Cu Kα radiation (λ =1.5418 Å, 30 kV, 40 mA, step 0.05° 2θ, time 1.5 s), connected to a DACO-MP microprocessor and using commercial Diffract-AT software. Diffraction

by line Kα$_2$ was removed using supplied software. The crystalline phases in the solids prepared were identified by comparison with the JCPDS files [12] and literature.

Differential thermal analyses (DTA) and thermogravimetric analyses (TG) were carried out in oxygen in DTA-7 and TG-7 instruments from Perkin Elmer, both connected to a PC, using Pyris software; heating was carried out at 10°C/min up to 1000 or 1200°C; derivative thermogravimetric (DTG) curves were obtained using the software provided.

The FT-IR spectra were recorded using the KBr pellet technique in a Perkin Elmer FT1730 spectrometer; 50 scans with a nominal resolution of 4 cm^{-1} were averaged to improve the signal-to-noise ratio.

Temperature-programmed reduction (TPR) analyses were carried out in a TPR/TPD-2900 instrument from Micromeritics, using H$_2$/Ar (5 vol.%) as reducing agent, at a heating rate of 10°C/min and using sample weights according to literature recommendations [13] to improve resolution of the peaks.

Adsorption-desorption isotherms of N$_2$ at -196°C for specific surface area and porosity assessment were recorded in a Gemini instrument from Micromeritics, using ca. 50-80 mg of sample previously degassed by flowing nitrogen at 110°C for 2-3 h in a Flow Prep instrument, also from Micromeritics.

RESULTS AND DISCUSSION

Element chemical analysis

Data are reported in table 1. The Co/Fe nominal ratios in the solids were very close to those expected from the amounts of reagents used to synthetise them, and the amounts of Co or Fe lost in the washing liquids were negligible, i.e., complete precipitation of the metal cations has been achieved. In addition, a small amount of sodium still exists in some of the samples, probably from incomplete washing. However, if the washing would be prolonged to fully eliminate sodium, pH decreases from the values reported in table 1; such a pH decrease could give rise to formation of interlayer hydrogencarbonate species instead of carbonate ones.

Table 1. Element chemical analyses for metals and other data on the preparation of the precursors.

Sample	Weight percentage			Co/Fe molar ratio		Washing liquids		
	Co	Fe	Na	Nominal	Experimental	Co (ppm)	Fe (ppm)	*pH*
CoFe01	32.22	15.79	n.d.	2.00	1.94	1.18	0.13	9.6
CoFe02	28.37	17.98	0.76	1.50	1.50	0.23	1.19	9.7
CoFe03	23.78	24.07	n.d.	1.00	0.94	0.30	1.70	9.4
CoFe04	20.17	29.96	0.12	0.67	0.64	0.20	0.70	9.5
CoFe05	15.98	32.73	0.25	0.50	0.46	0.75	0.79	9.4

n.d. = not detected

Powder X ray diffraction

The PXRD diagrams of all five precursors are shown in figure 1. The intensities and definition of the maxima decrease as the iron content increases (from top to bottom in the figure), although in all cases, the maxima recorded can be ascribed to diffraction by a LDH with the hydrotalcite-like structure. We will analyze in detail the diagram for sample CoFe01, that is, that with the sharpest diffraction maxima. The diagram is very similar to that previously reported for a CoFe hydrotalcite with a Co/Fe molar ratio close to 2.4 [11,14] and also containing carbonate as interlayer anion. Harmonics, which positions change only very slightly from one sample to another, are recorded at low 2θ values; the doublet close to $2\theta = 60°$ is also characteristic of the hydrotalcite structure, and it is well defined as the Co content increases. The position of the first maximum (ca. 7.7 Å), due to diffraction by planes (003) for a 3R packing of the brucite-like layers, has been used to calculate lattice parameter c as $c = 3 \cdot d(003)$, while parameter a, corresponding to the average closest metal–metal distance in the brucite-like layers, was calculated from the position of the first maximum of the doublet above mentioned at $d = 1.56$ Å, due to diffraction by planes (110), according to $a = 2 \cdot d(110)$ [15]. The lattice parameter values for all five samples are given in table 2. The value of c slightly decreases as the iron content increases, while the value of a remains constant. The value of c is related to the electrostatic interactions between the layers and the interlayer species; its variation amounts only 2 % from sample CoFe01 to sample CoFe05, so it can be assumed that these interactions have essentially the same strength in all five samples.

From the value of d(003) and the thickness of the brucite layer, 4.8 Å [16], the interlayer height is calculated as ca. 2.9 Å, consistent with location of carbonate ions with their molecular plane parallel to the brucite-like layers.

Table 2. Lattice parameters of the LDH phase in the precursors.

Sample	c (Å)	a (Å)
CoFe01	23.1	3.12
CoFe02	23.0	3.12
CoFe03	23.0	3.12
CoFe04	22.9	3.12
CoFe05	22.7	3.12

It should be noticed that, despite the hydrotalcite structure is usually assumed to be stable for M^{2+}/M^{3+} ratios equal or larger than 2 (i.e., that existing in sample CoFe01 if none of these cations undergoes red-ox processes during precipitation, washing or drying), no other crystalline phase is detected in our samples even when the iron content is increased, despite precipitation has been quantitative. Obviously, iron should be present in the form of amorphous hydroxides or hydrated oxides. Indexing of the diffraction maxima shown in figure 1 has been done using the formula by Gay [17] and from the c and a values calculated from the maxima ascribed to planes (003) and (110), respectively:

$$\frac{1}{d^2} = \frac{4(h^2 + hk + k^2)}{3a^2} + \frac{l^2}{c^2}$$

From the element chemical analyses data in table 1, the hydrotalcite-like structure of the solids, as concluded from the PXRD results shown in figure 1, the TG results (see below) and assuming carbonate as the only anion in the interlayer (according to the pH of the washing liquids and results from element chemical analyses), the chemical formula included in table 3 have been calculated for the compounds prepared. As the PXRD data indicate the presence of the hydrotalcite-like phase in all cases, the presence of this phase has been assumed with a nominal Co(II)/Fe(III) ratio of 2.0, which corresponds to the minimum value for a stable structure; in other words, assuming cobalt is the limiting reagent for the hydrotalcite-like structure formation, and so all
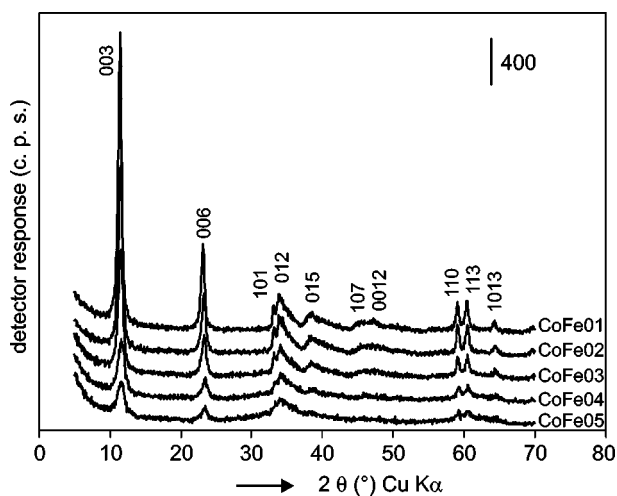

Figure 1. PXRD diagrams of the original samples. The diagrams have been vertically displaced for clarity. Labelled maxima correspond to diffraction planes of the hydrotalcite-structure.

Table 3. Chemical composition of the precursors*.

Sample	"dried" LDH	Fe_2O_3	H_2O
CoFe01	$[Co_{0.66}Fe_{0.34}(OH)_2](CO_3)_{0.17}$	-	0.50
CoFe02	$[Co_{0.67}Fe_{0.33}(OH)_2](CO_3)_{0.17}$	0.06	2.34
CoFe03	$[Co_{0.67}Fe_{0.33}(OH)_2](CO_3)_{0.17}$	0.19	4.35
CoFe04	$[Co_{0.67}Fe_{0.33}(OH)_2](CO_3)_{0.17}$	0.36	5.46
CoFe05	$[Co_{0.67}Fe_{0.33}(OH)_2](CO_3)_{0.17}$	0.55	13.25

all values have been rounded to two figures

cobalt existing in a given sample is forming a hydrotalcite-like structure. The iron in excess has been assumed to be as a hydrated oxide or oxohydroxide which precise chemical nature cannot be known from the data here reported, due to the low intensity and large broadness of their diffraction maxima; so, on describing the composition of the samples in table 3, all iron (in excess above the nominal hydrotalcite-like structure) it has been assumed to be as Fe_2O_3. The values for water content in table 3 correspond both to interlayer water in the hydrotalcite and hydration water of the iron oxides. The presence of these iron oxides would be also responsible for the rather broad diffraction at 2θ 33-36°, which intensity increases with the iron content.

Thermal studies

The DTG and DTA curves for all five samples, recorded in oxygen at a heating rate of 10°C/min up to 1000°C, are shown in figures 2 and 3, respectively; figure 2 also includes, as an inset, the TG curves.

Weight loss was ca. 30 % in all samples, slightly decreasing as the iron content was increased; in addition, the two Co-rich samples (CoFe01 and CoFe02) exhibit a clear weight loss at very high temperature, above 800°C, which is undetectable for the other samples. However, most of the weight is lost at a rather low temperature, and no more than 3% of the initial sample weight is lost above 300°C. The DTG curves indicate that sample CoFe01 behaves differently than the other samples. First of all, the weight losses take place at slightly higher temperatures; the first loss, below 100°C, is recorded as a mere shoulder to the main weight loss around 164°C, and a weight loss centered

around 226°C is not recorded for the other samples, although the main weight loss at 156°C for sample CoFe02 shows clearly a shoulder around 166°C. These two Co-rich samples exhibit, as mentioned above, a high temperature weight loss, at 886°C.

The DTA results are consistent with those reported by the TG/DTG study. Two endothermic effects are recorded below 300°C, which relative intensities change from one sample to another. So, the first effect, slightly above 100°C, recorded as a rather broad, medium strong, shoulder for sample CoFe01, shifts towards higher temperatures and strengthens with the iron content and is the main effect (albeit remaining rather broad), and is recorded at 133°C for sample CoFe05; in a parallel fashion, the second effect, at 190°C, becomes less intense in the same direction. This was the behaviour observed in the DTG curves. A tentative quantitative analysis indicates that the ratio between the areas of both DTA effects changes from ca. 1:5 for sample CoFe01 to 5:1 for sample CoFe05. Taking into account the phases detected by PXRD, we can safely assume that the first effect should be associated to removal of water, mainly from the amorphous hydrated iron containing components (which should be the major component in sample CoFe05), while the second one, which is much sharper, should be mainly related to removal of water from the hydrotalcite-like phase, both from the interlayer space and through condensation of hydroxyl groups of the layers. It should be also noticed that the DTA diagrams for the Co-rich samples show, in addition, a weak exothermic effect at 260-290°C, which can be ascribed to oxidation of Co(II) to Co(III) under the oxidizing conditions the analysis is carried out; its intensity drastically decreases as the Fe content is increased in samples CoFe03 to CoFe05, for which it is
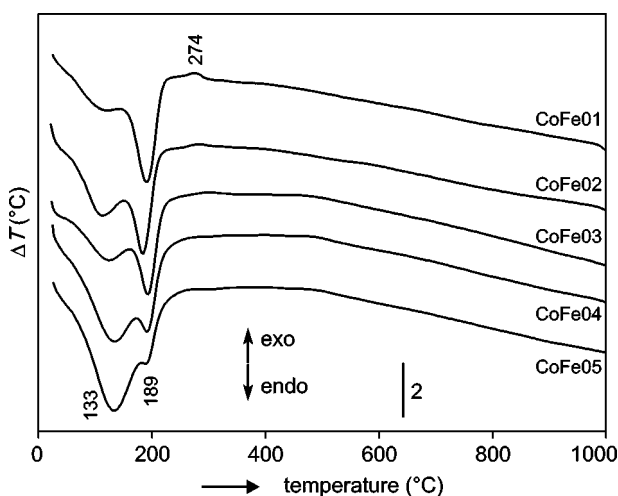

Figure 2. DTA curves of the samples recorded in oxygen. The curves have been vertically displaced for clarity.
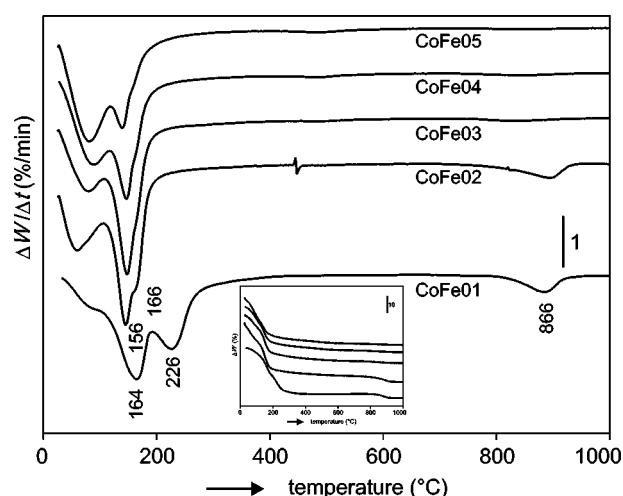
Figure 3. DTG curves of the samples. The curves have been vertically displaced for clarity. Inset: TG curves.

hardly detected. The reduction, again to the Co(II) state, of these Co(III) species, should be responsible for the high temperature weight loss recorded for samples CoFe01 and CoFe02 at high temperatures, above 850°C, in the TG curves. However, such a reduction process does not give rise to any detectable effect in the DTA curves.

Previous studies on samples to which those here studied are rather similar, but with a Co/Fe ratio between 2.4-2.7, showed also a single endothermic DTA peak when recorded in oxygen, with a second, weaker, endothermic peak, recorded at slightly higher temperature [11,14].

Although in some cases elimination of layer hydroxyl groups as water vapour is recorded at different temperatures than those for evolution of CO_2 from interlayer carbonate anions, in this case both processes occur simultaneously, and are not distinguished by these thermal methods.

Due to the steady changes in the behaviour shown by these five samples in the thermal study, a precise, quantitative analysis can be performed on the samples with the two wing compositions, i.e., CoFe01 and CoFe05.

The first main weight loss for sample CoFe01, up to ca. 400°C, corresponds to 28 % of the initial sample weight, and would correspond to removal of externally adsorbed and interlayer water molecules, together with water formed through condensation of layer hydroxyl groups and carbon dioxide from interlayer carbonate anions. Although evolved gases could not be analyzed in this case, previous studies [18,19] have shown that in this sort of compounds these species are removed in this temperature range. In addition, partial oxidation of Co(II) to Co(III) also takes place, as crystalline oxides containing Co(III) species were detected in the PXRD patterns of the solids calcined in oxygen at 400°C in the same conditions as those used to perform the TG and DTA studies. The high temperature weight loss amounts only 2.6 % of the initial sample weight for sample CoFe01, and corresponds to oxygen evolution due to partial decomposition of Co(III)-containing oxides, forming Co(II) species, as crystalline phases containing both species of cobalt have been identified in the residues after calcination.

The TG curve for sample CoFe05 shows only a single weight loss, which corresponds to 28 % of the initial sample weight (that is, coincident with the first weight loss for sample CoFe01, within experimental error). In this case, PXRD analysis of the residue after calcination indicates the presence of crystalline species containing exclusively Co(II) and Fe(III), so the Co(II) to Co(III) oxidation process, if any in these Fe-rich sample, has been completely reversed at high temperature.

FT-IR spectroscopy

The FT-IR spectra in the 2000-350 cm^{-1} range for the five solids are included in figure 4. In addition, all spectra show a broad, asymmetric band centered around 3430 cm^{-1}, due to OH stretching mode of hydrogen-bonded hydroxyl groups from the layers and the water molecules , and a broad shoulder at ca. 3200-2800 cm^{-1}, which has been previously attributed [20] to stretching mode of OH groups hydrogen-bonded to interlayer carbonate anions in the hydrotalcite-like structure; in agreement with the larger content of hydrotalcite in the Co-rich samples, this shoulder is only clearly detected for the Co-rich samples, CoFe01 and CoFe02. The medium intensity band close to 1635 cm^{-1} is due to the bending mode of water molecules.

The presence of interlayer carbonate species is clearly concluded from the couple of bands recorded at 1479 and 1352 cm^{-1}. Double degenerated mode v_3 of carbonate is recorded as a single band for the free ion [21]. As two bands are recorded for our samples, we should conclude that degeneration is cancelled because of a lowering in symmetry in the interlayer space of the
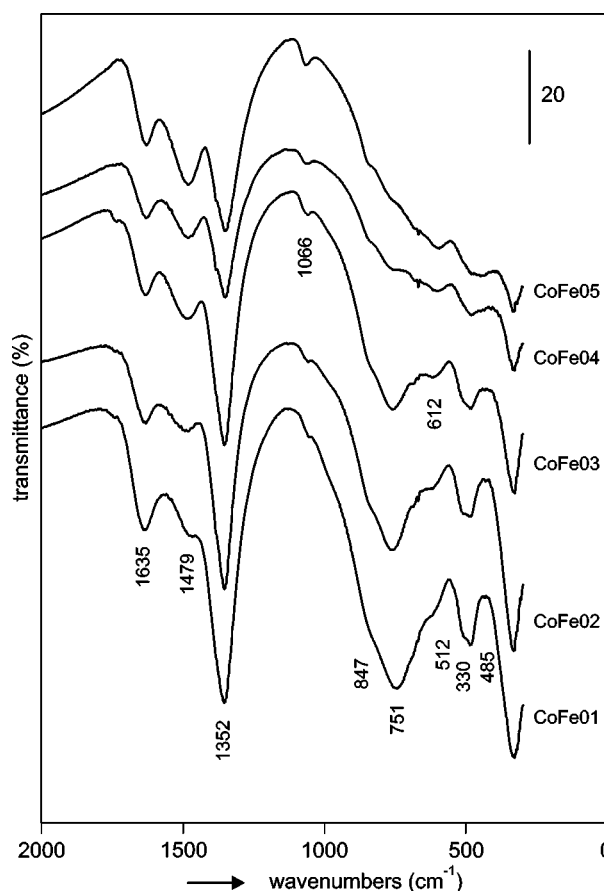

Figure 4. FTIR spectra of the original samples. The curves have been vertically displaced for clarity.

hydrotalcite structure, giving rise to the two bands mentioned. Moreover, it should be noticed that the relative intensities of these bands change with the Co/Fe ratio, the band at 1479 cm^{-1} becoming relatively stronger as the iron content increases, suggesting a more intense symmetry decrease. This should arise from the preferential interaction of the carbonate anions with "sites" in the layers closer to the location of the Fe(III) ions. A further confirmation of this stronger symmetry decrease when the iron content is increased comes from the development of a weak, but undoubtedly detectable, band at 1066 cm^{-1}, which intensity increases with the iron content. This band should be due to the completely symmetric ν_1 mode of carbonate, IR-forbidden for a regular D_{3h} symmetry (the free anion), but which becomes active for a lower symmetry, probably C_{2v}, through interaction of the carbonate with the layers. Mode ν_2 of carbonate should be responsible for the shoulder close to 847 cm^{-1} [22], while the band due to mode ν_4, which should be recorded at 685 cm^{-1} for CoFe hydrotalcites [23] is not recorded for these samples.

The other bands recorded in this low wavenumbers region are related to vibration modes involving layer cations. So, for CoFe hydrotalcites (to which our sample CoFe01 is similar), these bands are recorded at 770-764, 540-516 and 489 cm^{-1} [23,24]. In addition, a band at 337 cm^{-1} has been previously reported by Hansen et al. [23] as due to lattice vibrations in CoFe hydrotalcites; in the spectra of our samples, the intensities of all these bands decrease as the Fe(III) content is increased, i.e., as the hydrotalcite content decreases.

Temperature-programmed reduction

Reduction of CoFe hydrotalcites, under the experimental conditions here used, leads to complete reduction to Co(0) and Fe(0) [19,25]. In addition, carbon dioxide is removed before reduction to carbon or even hydrocarbons (possibly catalyzed by the layer cations) takes place, and so all hydrogen consumed during the experiments corresponds to reduction of the metal cations to the zero-valent state. The corresponding reaction can be written as:

$$Co^{II} + H_2 \rightarrow Co^0 + 2\ H^+ \tag{1}$$

$$Fe^{III} + 1.5\ H_2 \rightarrow Fe^0 + 3\ H^+ \tag{2}$$
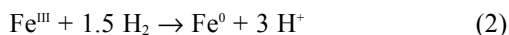
So, the amount of hydrogen to be consumed during the TPR experiments can be calculated from the knowledge of the concentration of metal cations in the different samples. In addition, reduction of some Co^{III} species formed through oxidation of the initially existing Co^{II} species can be written as:

$$Co^{III} + 1.5\ H_2 \rightarrow Co^0 + 3\ H^+ \tag{3}$$
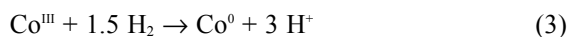
The extent of such an oxidation is unknown, but it can be qualitatively confirmed if the amount of hydrogen experimentally consumed is significantly larger than the theoretical amount corresponding to processes (1) and (2). However, it should be also noticed that the error usually admitted for this technique can be amount even 5-10 %, so small deviations cannot be safely taken as a quantitative indication of process (3).

The ratio between the experimental and the theoretically calculated amount of hydrogen consumed for reduction of the samples studied are summarized in table 4, and the corresponding TPR curves are included in figure 5. The named ratios range from 1.06 to 1.14, suggesting that a small portion of Co(II) has been oxidized to Co(III), but the results do not permit further refinement of the calculations to quantify the amount of Co(III) existing in the samples. On the other hand, as initial Fe(III) cannot be reduced to Fe(II) during synthesis, the amount of hydrogen theoretically consumed for process (2) could be taken from the Fe content, and
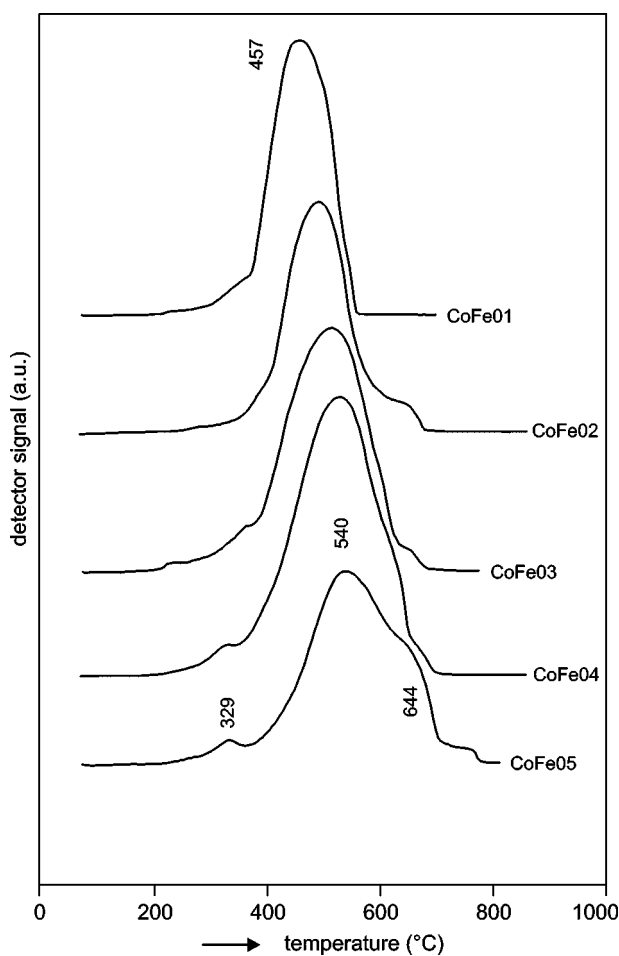
Figure 5. TPR curves of the original samples. The curves have been vertically displaced for clarity.

remaining hydrogen is ascribed to reduction of Co(II) and Co(III) to the zero valent state; as the stoichiometry of these two processes (1) and (3) above is known, the amount of Co(III) could be quantitatively determined. However, this would lead to wrong results, as all experimental error would be put on cobalt reduction. So, we think that the technique does not permit further calculation to "split" total hydrogen reduction into reduction of iron and reduction of cobalt separately.

Table 4. Temperature-programmed reduction and specific surface areas (m^2/g) results.

Sample	(exp/theoretical) H_2 consumption	S_{BET}
CoFe01	1.13	67
CoFe02	1.14	58
CoFe03	1.06	111
CoFe04	1.13	145
CoFe05	1.09	170
CoFe01/1200	1.19	a
CoFe02/1200	1.19	a
CoFe03/1200	0.98	a
CoFe04/1200	1.16	a
CoFe05/1200	1.15	a

a < 5 m^2/g in all cases

According to the curves in figure 5, reduction starts in all cases at 180-220°C and is completed at 550-780°C; the curve steadily shifts towards higher temperature as the iron content increases. For sample CoFe01 a single reduction band, with maximum at 457°C, is recorded, although an extremely weak reduction peak (more clearly recorded for sample CoFe05) is recorded at lower temperature; this small peak might correspond to reduction of Co(III) species, formed during drying of the samples, to Co(II). A clearly two-maxima curve (540 and 644°C) is recorded for sample CoFe05. For the samples with intermediate compositions it is clear that, in addition to the shift towards higher temperatures, the peak becomes broader, suggesting that two peaks exist in all five cases, probably corresponding to reduction of each of the metal cations. Reduction of single oxides indicate that Fe_2O_3 is reduced in two consecutive steps (probably due to Fe(III) → Fe(II) → Fe(0) processes), while CoO is reduced in a single step. It is also possible that once the first Co particles are formed, dissociative adsorption of hydrogen enhances reduction of the remaining oxidized species; as the Co content decreases, on passing from sample CoFe01 to sample CoFe05, such a process is somewhat hindered, and reduction starts at higher temperatures. This shifts permits isolation of the small reduction maximum above ascribed to Co(III) → Co(II) reduction, which is clearly recorded for sample CoFe05.

Surface texture

The nitrogen adsorption-desorption isotherms at -196°C correspond to type II in the IUPAC classification [26], and micropores seem to be absent. However, the intrinsic structure of these solids, with stacked layers, should contain micropores, but the width of the interlayer space (calculated from PXRD data as 2.9 Å) is too small to permit access of the nitrogen molecules to the interlayer space. All isotherms exhibit a hysteresis loop, which closes at a relative pressure of 0.4-0.5, which shape suggest the presence of particles with pores opened on both ends, which would correspond to the stacking of layered particles. The specific surface areas calculated following the B.E.T. method [27] are included in table 4. The value for sample CoFe01 is in the range usually found for this sort of samples submitted to similar preparation treatments [28]. With the exception of sample CoFe02 (which behaviour remains unexplained), a steady increase in the specific surface area is observed as the iron content is increased. This trend can be originated by the increasing content in amorphous iron oxides/hydroxides, with larger specific surface area than crystalline hydrotalcite, which concentration decreases as the iron content increases.

Calcined samples

As noted above, the solids were calcined in air at 1200°C for 1 h. Total weight loss upon calcination ranged from 29 to 32 %, depending on the specific sample. The specific surface areas of the calcined products were in all cases lower than 5 $m^2 g^{-1}$.

The PXRD diagrams for the calcined solids are included in figure 6. The sharpness and intensity of the diffraction maxima increase with the iron content and most of the peaks coincide with those reported in the JCPDS files with those of spinel $CoO \cdot Fe_2O_3$ (file 03-0864); actually, all peaks recorded in the PXRD diagram of sample CoFe05/1200 correspond to the named spinel, as expected bearing in mind that the molar Co/Fe ratio in this sample coincides with that existing in the spinel, if all Co is in the divalent state, in agreement with the TG results above given. From the positions of the diffraction maxima, the calculated lattice parameter for this spinel is $a = 8.31$ Å, which fits pretty well with the value reported [29] for $CoFe_2O_4$. The broad diffraction recorded in some cases is due to the glass sample-holder used.

For the Co-rich samples, in addition to the diffraction maxima of the spinel, other maxima can be ascribed to the presence of smaller amounts of CoO (file 09-0402) and probably Co_3O_4 (file 09-0418), that is in these Co-rich samples the thermal treatment has not been strong enough to reduce all cobalt to the divalent state.
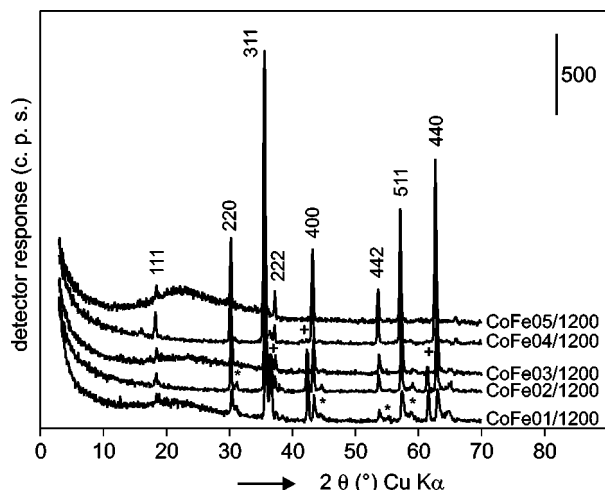
Figure 6. PXRD diagrams of the samples calcined in air at 1200°C. Labelled maxima correspond to diffraction planes of the spinel structure. (*) peaks due to Co_3O_4 (JCPDS file 09-0418); (+) peaks due to CoO (JCPDS file 09-0402). The curves have been vertically displaced for clarity.

The FTIR spectra of the calcined products, figure 7, do not exhibit any absorption band which could be ascribed to the presence of carbonate species; however, a medium intensity, broad, band is recorded around 3400 cm^{-1}, due to the stretching mode of OH species in water molecules, adsorbed probably on the external surface of the samples during handling to record the spectra. The band corresponding to the bending mode is recorded at ca. 1640 cm^{-1}. In the low wavenumbers region the main band is recorded at ca. 570 cm^{-1}, more clearly in sample CoFe05/1200, but with a well defined shoulder at 644 cm^{-1} for sample CoFe01/1200; the intensity of this shoulder decreases as the iron content is increased, and is totally absent in the spectrum of sample CoFe05/1200. The band at 570 cm^{-1} is associated to the presence of the $CoO \cdot Fe_2O_3$ spinel, while the band at 644 cm^{-1} should be due to the presence of the cobalt spinel, undoubtedly identified in the PXRD diagrams of the Co-rich samples. Bands due to the deformation modes of these species are hardly recorded at lower wavenumbers.
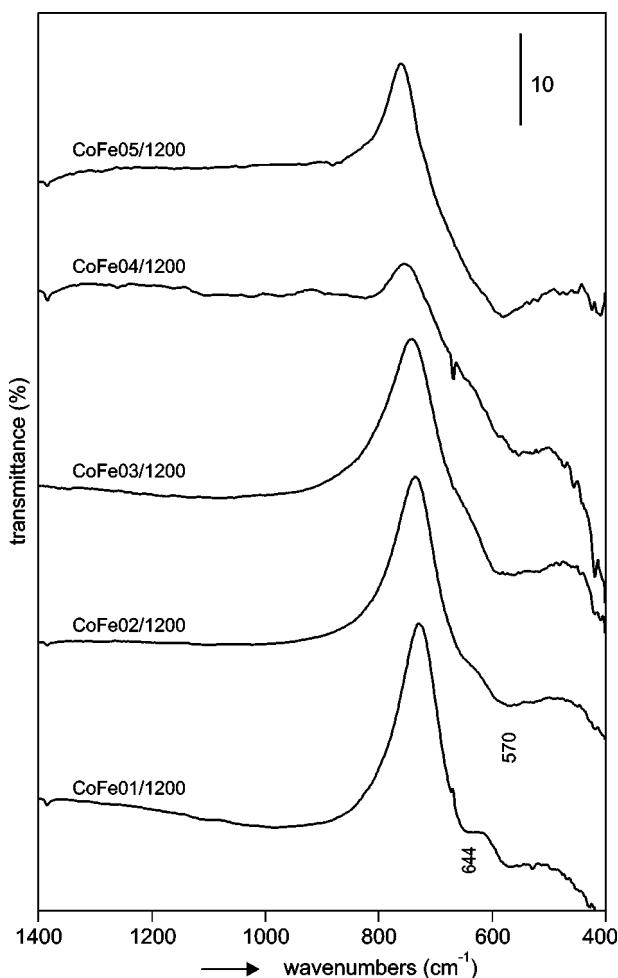

Figure 7. FTIR spectra of the samples calcined in air at 1200°C. The curves have been vertically displaced for clarity.
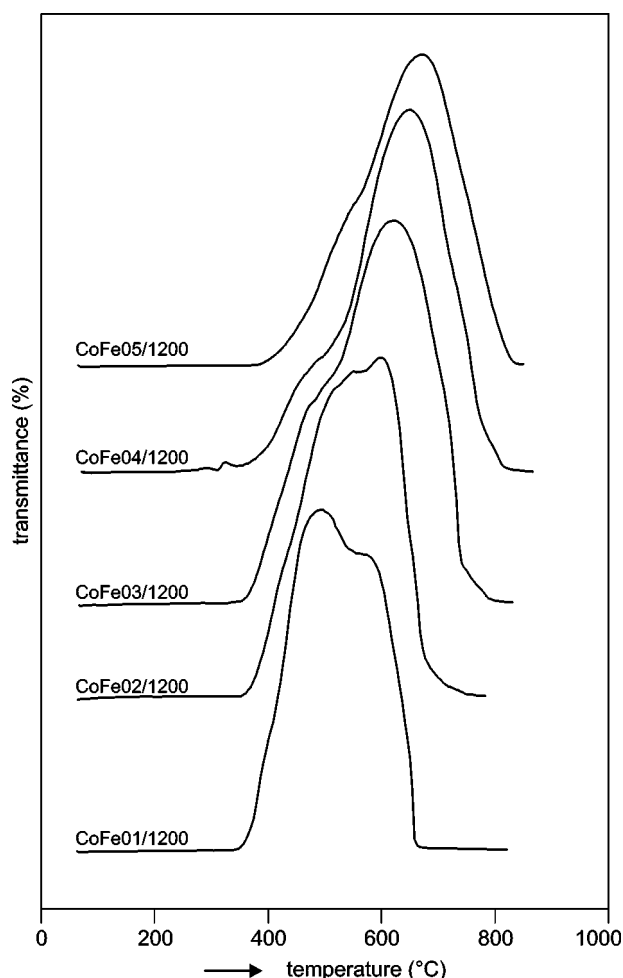

Figure 8. TPR curves of the samples calcined in air at 1200°C. The curves have been vertically displaced for clarity.

Finally, the TPR curves for the calcined samples are included in figure 8; the corresponding data concerning the ratio between the amount of hydrogen consumed (experimental/theoretical) are included in table 4. As for the uncalcined samples, the position of the maxima shift to higher temperature as the iron content is increased. Such a shift is even more marked for the Fe-rich samples. A two-steps reduction is observed for sample CoFe01/1200 (a single, albeit broad, peak was recorded for the corresponding uncalcined sample, see figure 5). Such a shift can be attributed to two different origins: first of all, the nature of the species being reduced is different in the calcined or in the original samples; secondly, the calcined samples are very crystalline, and reduction should be more difficult, probably because of difusion control. Looking at the TPR curves, figure 8, it seems that the position of the first component of the doublet for sample CoFe01/1200 remains almost unchanged for the different samples, although its intensity decreases when the iron content is increased; this behaviour suggests that such a reduction maximum is due to consumption of hydrogen for cobalt reduction. On the contrary, the second maximum shifts gradually to higher temperatures. The values reported in table 4 for hydrogen consumption are rather similar to those calculated for the uncalcined samples, and, within experimental error, are due to processes (1) and (2) above described, that is, the Co(III) content in the Co-rich, calcined samples should be rather low if compared with Co(II).

CONCLUSIONS

Quantitative synthesis of CoFe-carbonate layered double hydroxide and of its mixtures with hydrated iron oxides has been achieved by precipitation at constant pH. Depending on the molar Co/Fe ratio, a pure LDH or mixed phases are obtained. On calcination at high temperature a pure crystallographic spinel phase is obtained when the Co/Fe molar ratio is 1/2, where all cobalt is in the +2 state; samples with larger Co/Fe ratio contain also different amounts of Co_3O_4 and of CoO, which formation takes place even under oxidizing conditions between 800-900°C. The method used permits synthesis of tailored mixed oxides.

Acknowledgement

References

1. Rives V.: *Layered Double Hydroxides: Present and Future*, Nova Sci., New York 2001.
2. Rives V., Ulibarri M.A.: Coord Chem.Rev. *181*, 61 (1999).
3. Newman S.P., Jones W.: New J.Chem. p. 105, (1998).
4. Cavani, F., Trifiro, F. Vaccari A.: Catal.Today *11*, 173 (1991).
5. Vaccari A.: Appl. Clay Sci. *14*, 161 (1999).
6. de Roy A., Forano C., Besse J.-P. in: *Layered Double Hydroxides: Present and Future*, p. 1-37, Ed. Rives V., Nova Sci., New York 2001.
7. Basile F., Vaccari A. in: *Layered Double Hydroxides: Present and Future*, p. 285-321, Ed. Rives V., Nova Sci., New York 2001.
8. Monzón A., Romeo E., Marchi A.J. in: *Layered Double Hydroxides: Present and Future*, p. 323-382, Ed. Rives V., Nova Sci., New York 2001.
9. Rives V., Dubey A., Kannan S.: Phys.Chem.Chem. Phys. *3*, 4826 (2001).
10. Dubey A., Rives V., Kannan S.: J.Molec.Catal. A: Chemical *181*, 151 (2002).
11. del Arco M., Trujillano R., Rives V.: J.Mater.Chem. *8*, 761 (1998).
12. JCPDS: Joint Committee on Powder Diffraction Standards, International Centre for Diffraction Data, Pennsylvania, U.S.A. 1977.
13. Malet P., Caballero A.: J. Chem. Soc., Faraday Trans. I *84*, 2369 (1988).
14. R. Trujillano, Ph. D. Thesis, University of Salamanca, Salamanca, Spain, 1997.
15. Drits V. A., Bookin A.S. in: *Layered Double Hydroxides: Present and Future*, p. 39-92, Ed. Rives V., Nova Sci., New York 2001.
16. Miyata S., Okada A.: Clays Clay Miner. *25*, 14 (1977).
17. Gay P.: *The Crystalline State. An Introduction*, 3rd ed., Oliver & Boyd, Edinburgh 1972.
18. Rives V.: Inorg.Chem. *38*, 406 (1998).
19. Rives V. in: *Layered Double Hydroxides: Present and Future*, p. 115-137, Ed. Rives V., Nova Sci., New York 2001.
20. Kruissink E. C., van Reijden L. L., Ross J.R.H.: J.Chem.Soc., Faraday Trans. I *77*, 649 (1981).
21. Nakamoto K.: *Infrared and Raman Spectra of Inorganic and Coordination Compounds*, 5th ed., John Wiley & Sons, New York 1997.
22. Kloprogge J. T., Frost R. L. in: *Layered Double Hydroxides: Present and Future*, p. 139-192, Ed. Rives V., Nova Sci., New York 2001.
23. Hansen H. C. B., Koch C. B., Taylor R. M.: J. Solid State Chem. *113*, 46 (1994).
24. Zeng H. C., Xu Z. P., Qian M.: Chem.Mater. *10*, 2277 (1996).
25. Rives V., Ulibarri M. A., Montero A.: Appl. Clay Sci. *10*, 83 (1995).

26. Sing K. S. W., Everett D. H., Haul R. A. W., Moscou L., Pierotti R., Rouquerol J., Sieminiewska J.: Pure Appl. Chem. *57*, 603 (1985).
27. Lowell S., Shields J. E.: *Powder Surface Area and Porosity*, Chapman & Hall, London 1984.
28. V. Rives in: *Layered Double Hydroxides: Present and Future*, p. 229-250, Ed. Rives V., Nova Sci., New York 2001.
29. Greenwood N. N.: *Ionic Crystals, Lattice Deffects and Non Stoichiometry Butterworth*, Chapman & Hall, London l968.

PŘÍPRAVA A VLASTNOSTI SMĚSNÝCH OXIDŮ Fe A Co PŘIPRAVENÝCH Z VRSTEVNATÝCH PODVOJNÝCH HYDROXIDŮ

MARÍA E. PÉREZ BERNAL, RICARDO J. RUANO CASERO, VICENTE RIVES

Departamento de Química Inorgánica
Universidad de Salamanca, 37008-Salamanca, Spain

Tuhé látky obsahující Co(II) a Fe(III) v molárním poměru 2:1, 3:2, 1:1, 2:3 a 1:2 byly připraveny spolusrážením při konstantním *pH*. Všechny měly strukturu hydrotalcitu s uhličitanovým aniontem v mezivrstvě a s krystalinitou klesající s rostoucím obsahem železa. Jiné fáze nebyly zjištěny dokonce ani ve vzorcích s nejvyšším obsahem F. Vzorky byly charakterizovány práškovou rtg difrakcí, FT IČ spektroskopií, termální analýzou (diferenční termální analýzou, termogravimetrií a tepelně programovanou redukcí), a dále měřením specifického povrchu adsorpcí dusíku při -196°C. Ve vzorcích bohatých Co byla pozorována mírná oxidace Co(II) a Co(III), přičemž Co(II) je obnoven po kalcinaci na asi 850°C v kyslíku. Tepelný rozklad probíhá v jediném kroku kolem 350°C a specifický povrch roste s rostoucím obsahem železa, pravděpodobně díky přítomnosti hydratovaných amorfních oxidů Fe. Fáze zahřívané na 1200°C na vzduchu obsahují krystalický CoO, Co_3O_4 a $CoFe_2O_4$ (spinel); spinel je ve vzorcích převažující fází a při vysokém obsahu Fe fází jedinou. Kovové ionty jsou snáze redukovatelné v původních než v kalcinovaných vzorcích, a ve všech vzorcích se železo patrně redukuje při vyšší teplotě než kobalt.

Book review

PROGRESS IN BIOCERAMICS. A PROGRESS IN CERAMIC TECHNOLOGY SERIES BOOK

Geiger G. (editor)

Published by The American Ceramic Society, 735 Ceramic Place, Westerville, Ohio 43081, USA, 2004; ISBN: 1-57498-193-5, price 109,- USD (87,- USD ACerS Members)

The reviewed book, which is the new issue of "A Progress in Ceramic Technology Series", is a compilation of recent scientific papers concerned in glass and ceramic materials used in medicine. All articles included in the book originated from journals and proceedings published by The American Ceramic Society (ACerS), namely from The Journal of American Ceramic Society (JACS), American Ceramic Society Bulletin (ACSB), Ceramic Transaction (CT) and Ceramic Engineering and Science Proceedings (CESP).

Papers involved in this compilation are mostly from the years 2002-2004 and the book is a good starting point for the basic literature research in the field of biomaterials. The lead-off article by Larry L. Hench was published in 1998 as a centennial feature article. However, it is the excellent overview of the biomaterials and it can be recommended as an introductory text for postgraduate student starting in the study programmes oriented on biomaterials.

At 342 pages, 50 articles are involved in the book, 26 reprinted from JACS, 3 from ACSB, 5 from CT and 16 from CESP. Formally, the book is divided into four parts according to the original publication of articles. This arrangement could be the only one objection to the reviewed book. It would be more comfortable for readers to obtain the book divided according to material types or by another point of view - for example preparation, testing, structure etc.

Finally, it can be summarised that the reviewed book can help as the starting point for the fast literature search and the first paper with overview by L.L. Hench is a good basis for postgraduate students' introduction into the field of biomaterials. It is only a pity that there are not involved papers published in European journals. We can only hope the European publishers will also follow this activity and that the similar compilation will be prepared from other journals.

As any book published by The American Ceramic Society it can be ordered using the on-line catalogue www.ceramics.org.

Aleš Helebrant